

Conversion of Gaseous Hydrocarbons in Cold Electron-Beam Plasma

R. G. Sharafutdinov^{a, *}, V. O. Konstantinov^a, V. I. Fedoseev^a, V. G. Shchukin^a, and S. A. Gorodetskii^a

^a*Kutateladze Institute of Thermal Physics, Siberian Branch, Russian Academy of Sciences, Novosibirsk, Russia*

**e-mail: molkin@itp.nsc.ru*

Received October 23, 2018; revised February 11, 2019; accepted February 15, 2019

Abstract—A new method for plasma-assisted reforming of hydrocarbon gases is briefly described, and the results of oxidative (without the synthesis gas stage) and nonoxidative conversion to new gaseous and liquid products are exemplified. The method is based on the unique property of cold plasma, the dramatic acceleration of chemical processes due to the plasma activation of particles, which makes it possible to enhance reactions in small flow reactors without the use of catalysts.

Keywords: plasma-assisted reforming of natural gas, electron-beam plasma, cold plasma generator

DOI: 10.1134/S0965544119130127

The cost-effective processing of gaseous hydrocarbons into useful products—there are many of them, such as liquefied gas, synthesis gas, methanol, hydrogen, acetylene, ethylene, and other products with high added value—is a very urgent task. This task is divided into two classes, the processing of natural gas (NG) and associated petroleum gas (APG) produced in large fields and small off-balance fields. For the second class of natural gas sources, the construction of large gas processing plants is unprofitable and on-site gas processing is necessary.

The requirements for small-scale production gas chemistry are perfectly set forth in the paper by Arutyunov and coworkers [1]. Without dwelling on these requirements in detail, we note that the main one is the need to create transportable miniplants for on-site gas processing. This condition, in turn, can be satisfied only at the highest rate of chemical reactions, which is unattainable with thermal and catalytic activation of processes. Cold and, as a result, highly non-equilibrium plasma has a chance to become the main type of plasma for designing modular, mobile units for processing hydrocarbon gases into useful products. Electron-beam plasma, which is the subject of this study, refers to this type of plasma.

The aforementioned chance is due to several factors. The first of them is that chemical reactions in a chemically active plasma proceed at the highest rate appropriate for the design of compact equipment with a sufficiently high productivity. The explanation for this acceleration of chemical reactions is that the species generated in a plasma (vibrationally excited molecules, radicals, ions, etc.) interact with each other, as well as with unexcited particles, in a different way than in the case of thermal activation. The rates of chemical reactions during plasma activation are several orders of

magnitude higher than in the case of thermal activation [2]. This acceleration of reaction rates is similar to catalytic, but unlike conventional catalysis in which reactions occur on the catalyst surface, plasma-induced reactions occur in the entire reactor space and involve simultaneously all species in the reactor; moreover, this reactor is a continuous-flow device. The flow rates of the reacting gas are not limited by the rates of chemical reactions, which are very high, so the residence time of the reacting species in the reactor can be very short.

The second, no less important factor leading to the highest reaction rates is the absence of significant heating of the gas in cold plasma, unlike the case of arc plasma. The consequence of this, in accordance with the Arrhenius law, is the freezing of reverse chemical reactions, which dramatically increases the useful yield of the product.

A technological benefit due to the above factors is a sharp increase in the specific productivity of the equipment, that is, productivity per unit volume of the reaction zone [3]. In addition, the low temperature of the process weakens the requirements for structural materials; increases the service life of the equipment; reduces heat exchange with the surroundings; and, finally, allows operation with any medium, including corrosive ones.

This raised the question of why, with such obvious advantages, cold plasma has not been actively used in gas processing, except electron-beam cleaning of flue gases [4–6]. The first reason is that cold plasma must be arranged in flow systems at industrially acceptable plasma gas flow rates. Second, the specific energy inputs achieved to date for a particular product (hydrogen, acetylene, synthesis gas, etc.) in laborato-

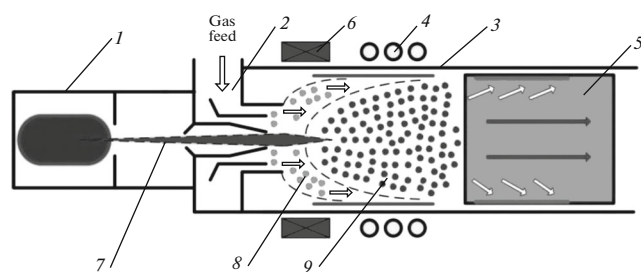


Fig. 1. Schematic of the plasma reactor: (1) hollow-cathode electron gun, (2) block of annular Laval nozzles, (3) reactor, (4) device for supplying power from an external electromagnetic field, (5) separator, (6) system of electromagnets, (7) electron beam, (8) not activated gas jets, and (9) chemically active electron-beam plasma.

ries, although quite low from the standpoint of industrial application, have not been confirmed for feed flow rates on the industrial scale, and even the trends of experimental, laboratory dependences are not clear for extrapolating to industrial flow rates. An overview of the use of cold plasma, including electron-beam plasma, can be found in [7–10].

To solve the first problem (increasing the productivity of plasma-chemical equipment and its service life), a cold plasma generator was designed [11]. It consists of a special electron gun, a gas shutter, and a block of annular nozzles, differing from the arc plasma torch by a significantly lower temperature of translational degrees of freedom of generated active heavy particles (atoms, molecules, radicals, etc.) [12]. An electron beam forms an electron-beam plasma in the reactor space, and the gas shutter allows the electron beam to the volume of the plasma reactor with a pressure at the reactor outlet up to atmospheric and gas flow rates through it of at least 1000 m³/h. The gas shutter is a very compact device, in contrast to the gateway systems that are traditionally used to extract an electron beam from the electron gun body.

To solve the second problem (reducing specific energy consumption for plasma-chemical conversion) is the aim of this study, the essence of which is a more complete, optimal use of electrons generated in electron-beam plasmas.

PLASMA JET TECHNIQUE

The basic unit of the plasma jet process is the reactor. Figure 1 shows a diagram of the plasma reactor with electron-beam activation. The reactor unit consists of electron gun 1, block of annular nozzles 2, the reactor per se 3, device 4 for supplying power from an external electromagnetic field, and separator 5 for collecting the products.

The electron gun serves to form electron beam 7. The block of annular nozzles has a dual function: to feed working gases through it and to serve as a gas

shutter maintaining the differential pressure in the electron gun and the reactor. The reactor itself is the volume in which chemical reactions proceed to give useful products. For additional, more effective activation, an external electromagnetic field is used that accelerates slow secondary electrons of the electron-beam plasma. To change the trajectory of the secondary electrons, expressed in their twisting in the direction perpendicular to the gas flow, a system of electromagnets 6 is installed.

Working gases, methane, NG, APG, and other hydrocarbon gases are supplied to the external nozzle of the nozzle block, and shielding gas is supplied through the internal nozzle of this block. In oxidative conversion, oxygen, carbon dioxide, and steam can be used as an oxidizing agent. The pressure difference between the braking pressure in the prechambers of the annular nozzles (internal and external) and the pressure at the section of Laval nozzles is chosen so as to provide supersonic gas flows at the edge of the nozzles. This condition is necessary to ensure the operation of the nozzle block as a gas shutter.

The electron beam 7 formed in the electron gun passes through the central hole of the nozzle block and enters into gas jets 8, which are formed behind the edge of the annular nozzles. On this structurally complex gas jet (gas target), the electron beam is scattered. The electron-beam energy is distributed into ionization to generate secondary electrons; dissociation; and excitation of internal degrees of freedom of atoms, molecules, and radicals. Thus, chemically active electron-beam plasma 9 is formed. Chemical reactions involving both plasma-induced active species and nonactivated particles occur in this plasma. The products formed in the plasma are carried over by the gas-plasma flow into the separator. To additionally increase the energy of secondary electrons and change the shape of the distribution function, an external field 4 is applied to the electron-beam plasma.

In the nonequilibrium cold plasma under consideration, the energy of electrons is consumed primarily for the activation of feedstock molecules. Gas heating (energy transfer from electrons to the translational degrees of freedom of atoms and molecules) is small—this is due to the cross sections of processes. Gas heating can result from relaxation processes, energy transfer from internal degrees of freedom to the translational motion of gas molecules. Therefore, the degradation of the resulting desired products is small due to the low temperature of the gas. This feature strongly distinguishes cold plasma from thermal plasma, where the gas temperature is high. An important advantage of a cold plasma generator is the ability to operate with any working gases, including aggressive ones.

In the described type of device, the generation of chemically active plasma occurs within a very short period of time on the order of 10⁻⁶ s and secondary reactions, due to their highest rate, occur over times

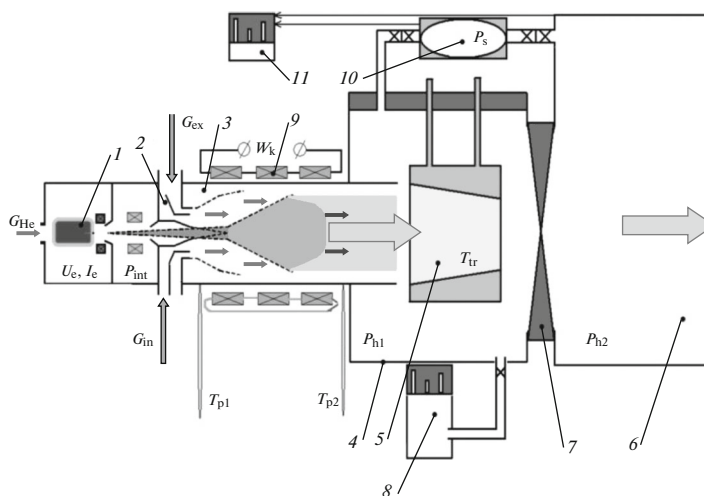


Fig. 2. Block diagram of the setup: (1) electron gun, (2) block of annular nozzles, (3) reactor, (4) vacuum chamber of the “Test Bench”, (5) nitrogen trap, (6) vacuum station chamber with a receiver, (7) vacuum shutter, (8) mass spectrometric system, (9) external electromagnetic field, (10) sampler, and (11) chromatograph.

on the order of one microsecond. It is very important that in this device, unlike arc plasma torches, plasma is formed directly in the reactor volume.

EXPERIMENTAL

The experiments on the conversion of hydrocarbon gases were carried out on the “Test Bench” setup of the Institute of Thermal Physics, SB RAS. The block diagram of this setup is shown in Fig. 2. Table 1 details the notations of this figure and presents ranges within which the determining parameters of the conversion process have changed.

The main elements of the setup are electron gun 1, nozzle block 2, reactor 3, “Test Bench” vacuum chamber 4, nitrogen trap 5, vacuum station chamber 6 with a receiver, vacuum shutter 7 connecting the vacuum station to the Test Bench chamber, mass-spectrometric system 8, external electromagnetic field 9, sampler 10, and chromatograph 11.

The working gases were fed into the chamber of the external Laval nozzle of nozzle block 2 and then into the volume of plasma reactor 3. The shielding gas (most frequently, helium) was supplied through the internal nozzle of this unit. The difference between the pressure in the prechambers of the nozzle block and the pressure at the exit of the Laval nozzles was maintained by pumping through a vacuum station shutter to ensure supersonic flows at the edge of these nozzles. The electron gun space and the intermediate pumping section (not shown in Fig. 2) were pumped out by independent vacuum systems.

The experiments were carried out in the following order. An electron beam formed in the electron gun was introduced through the central hole in nozzle block 2 into plasma reactor 3. Interacting with gas

flows in the volume of this reactor, the beam transferred its power ($I_E \times U_E$) to the gas jet to generate a chemically active plasma in which chemical reactions proceeded. The products of these reactions were collected in trap 5 cooled with liquid nitrogen. The freezing process continued for a few tens of minutes. During the experiment, mass-spectrometric determination of the product composition was carried out. For this purpose, mass-spectrometric system 8 was connected via a leak valve to the volume of vacuum chamber 4 of the laboratory test bench. After the experiment, the vacuum chamber of the bench was cut off by shutter 7 from the vacuum station, and the nitrogen trap was thawed.

Evaporation of frozen products with increasing temperature led to an increase in pressure P_H^1 in the “Test Bench” volume. The pressure increment after thawing was a measure of the amount of frozen product. The composition of this product was determined both mass spectrometrically and chromatographically. For chromatographic measurements, the gas after defrosting the nitrogen trap was refrozen in sampler 10 and then sent to chromatograph 11 to determine the composition of the obtained liquid.

An example of the results of mass-spectrometric determinations is given in Table 2. The table presents the data obtained in the mode of oxygen-free reforming. For comparison, Table 2 shows the mass spectrum measured in the laboratory setup of the initial dry natural gas, as well as the NIST standard mass spectrum of methane CH_4 and experimental data from other authors [13].

As can be seen, the mass spectrum of the reactant agrees well with the NIST data: it mainly contains methane lines (C^+ , CH^+ , CH_2^+ , CH_3^+ , CH_4^+) at m/z 12

Table 1. Details of the notations of Fig. 2 and ranges of variation of determining parameters

No.	Unit of setup	Determining process parameter	Designation of process parameter	Parameter variation range
1	Electron gun (EG)	Helium flow rate	G_{He}	0–50 sccm
		EG accelerating voltage	U_e	0.5–4 kV
		EG electric current	I_e	100–700 mA
		Pressure in intermediate section	P_{int}	10^{-4} – 10^{-1} Torr
2	Nozzle block	Gas flow rate through internal nozzle	G_{in} (CH ₄) + $G(\text{oxid})$	1–20 L/min
		Gas flow rate through external nozzle	G_{ex} (CH ₄) + $G(\text{oxid})$	5–100 L/min
3	Reactor	Temperature of magnets	T_m	300–400 K
		Reactor temperature	T_{p1}, T_{p2}	300–900 K
4	Vacuum chamber of “Test Bench”	Background pressure	P_{h1}	10^{-3} Torr
5	Nitrogen trap	Nitrogen trap temperature	T_{tr}	50–300 K
6	Vacuum chamber with receiver	Chamber pressure	P_{h2}	10^{-4} – 10^{-1} Torr
7	Vacuum shutter	Differential pressure	ΔP	10^{-4} – 10^{-1} Torr
8	Mass spectrometric system	Pressure in detector section	P_d	10^{-5} – 10^{-1} Torr
		Pressure in mass spectrometer section	P_{ms}	10^{-8} – 10^{-4} Torr
		Pressure in nitrogen trap of detector	P_{nt}	10^{-7} – 10^{-1} Torr
9	External electromagnetic field	Discharge voltage	U (low-temperature glow discharge)	0–450 V
		Effective discharge current	I_{eff} (low-temperature glow discharge)	0–20 A
		Microwave power	W_k (MW discharge)	0.2–2 kW
10	Sampler	Pressure in sampler after sampling	P_s	0–3 atm

Table 2. Comparative data of methane mass spectrometry in relative units (abundance at mass number 16 is taken as 100%)

Atomic mass unit	Methane without plasma	Methane according to NIST	Published data [13]	Methane in plasma (example)
16	100.00	100.00	100.00	100.00
15	85.00	87.71	88.72	78.30
14	16.50	21.14	17.46	15.60
13	8.90	10.15	9.48	9.10
12	2.70	4.24	3.61	2.59
2	0.98	0	0.48	12.40

to 16, respectively, and there is a small peak at m/z 1 due to atomic hydrogen. There are no peaks at other m/z values in the recorded mass spectrum of the reactant (at the detection limit of the mass spectrometer used).

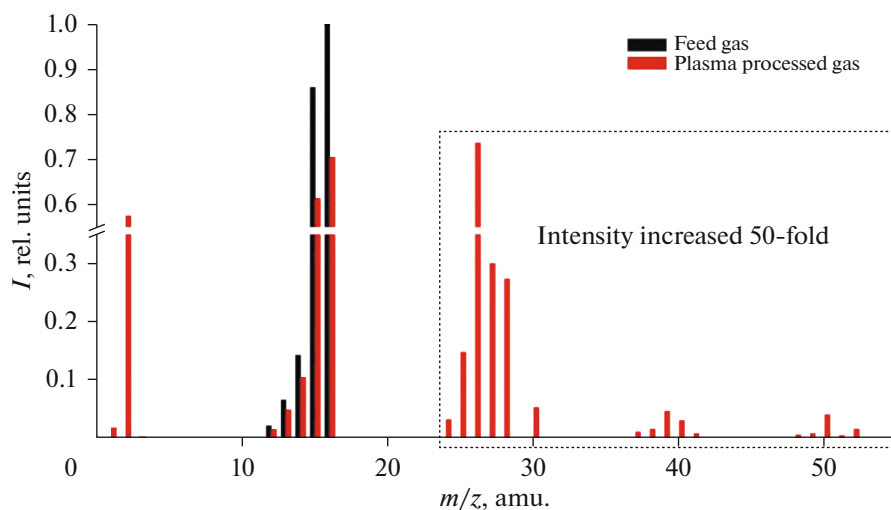
The mass spectrum of the gas after plasma treatment has a completely different pattern as shown in Fig. 3 and column 1 of Table 3. As can be seen, there is an intense peak of molecular hydrogen (m/z 2); the intensity of all methane lines decreased; and new lines appeared in the mass-to-charge ranges of 24–30, 37–41, and 48–52. For clarity, Fig. 3 collates the mass spectra after plasma processing and the mass spectrum of the reactant.

A preliminary interpretation of the obtained mass spectra using standard mass spectra demonstrates the appearance of new products in the composition of plasma-processed gases. The tentative composition of these products according to this mass spectrum is given in Table 3. All new products, such as molecular hydrogen and acetylene, are the result of plasma-chemical reactions initiated by plasma activation of the feed gas, indicating that despite the low gas density in laboratory experiments and the very short residence

time of the gas in the reactor because of the high gas flow rate in the reactor of a short length, reactions yielding the new products have time to proceed. This fact confirms the basic idea of cold plasma chemistry about the highest rate of chemical reactions involving active species.

Figure 4 shows the mass spectra of liquid products collected in the sampler after plasma treatment of natural gas and, in addition, the mass spectrum of the feedstock gas composed of 95% methane and 5% propane–butane mixture. The mass spectrum of the feed gas shows the presence, in a small amount in comparison with the liquid product of plasma processing, of groups with an m/z value in the range of C_1 – C_3 ; they correspond to fragments of heavier hydrocarbons present in the feed natural gas. The mass spectrum of the liquid exhibits groups of lines corresponding to carbon numbers from C_1 to C_6 . Apparently, there are also groups with C numbers greater than C_6 , but these m/z values are beyond the range of detection of the mass spectrometer used.

All groups of mass-spectrometric peaks in the sample (liquid sample) obtained by plasma processing of the reactant gas mixture are significantly higher in

**Fig. 3.** Mass spectrum for the case of plasma processing of natural gas.

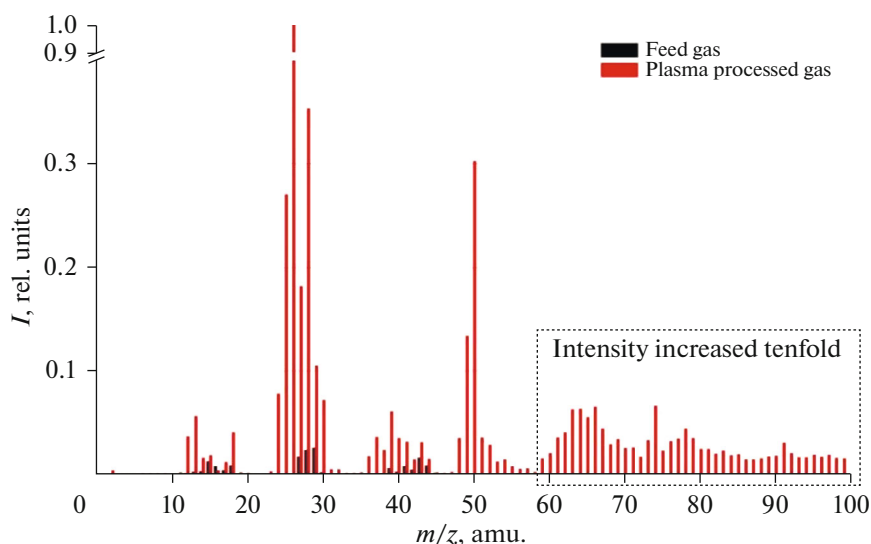


Fig. 4. Mass spectrum of liquid products of natural gas reforming.

intensity than in the control sample. Consequently, in the reactor during plasma-assisted conversion, processes are taking place to yield new hydrocarbons with a greater carbon number than in the reactant; i.e., there is catalytic reforming of light into heavier hydrocarbons, including liquid products. Below, Table 4 presents data of the gas chromatographic–mass spectrometric analysis of the liquid phase obtained in one of the experiments on the oxidative conversion of methane.

The measurements were made using a ZB-WAX column, 30 m × 0.32 mm × 10 μm (conditions: starting at 60°C with holding for 3 min and subsequent heating to 250°C at a rate of 9°C/min). A semiquantitative composition without water and methanol was

Table 3. Mass spectrometrically determined composition of the gas fraction of the products of plasma-chemical reactions

Product	Concentration in gaseous sample, %
Hydrogen (H ₂)	17.5
Methane (CH ₄)	70.0
Acetylene (C ₂ H ₂)	1.4
Ethylene (C ₂ H ₄)	0.6
Ethane (C ₂ H ₆)	0.2
Cyclopropene (C ₃ H ₄)	0.2
1,3-Butadiene (C ₄ H ₂)	0.2
Not identified	9.9

determined. The percentage of substances in the sample can be calculated by multiplying the peak area of a particular substance by 0.44. Evaluation of the methanol content by the additivity method gives 56%.

As can be seen from Table 4, plasma-assisted reforming opens up the opportunity to obtain a very wide variety of useful chemical products, with the product selectivity being very high, unattainable in the case of catalytic reforming or partial oxidation in a single-pass mode.

CONCLUSIONS

The plasma-assisted noncatalytic reforming of hydrocarbon gases to useful products in the mode of conversion with or without oxygen has been demonstrated. The highest rate of chemical reactions in the gas activated in cold nonequilibrium plasma makes it possible to run the conversion of hydrocarbon gases in compact, modular units suitable for on-site feedstock processing. The plasma-assisted reforming process depends on a very large number of determining parameters; therefore, its optimization requires the knowledge of the dependences on these parameters, which can be revealed using a cold plasma generator, a device described in this paper. Description of optimization of plasma-assisted reforming of hydrocarbons is the subject matter of the forthcoming papers.

CONFLICT OF INTERESTS

The authors declare that there is no conflict of interest requiring disclosure in this article.

Table 4. Composition of the liquid fraction of the products of plasma-chemical reactions

Peak	Peak elution time, min	Peak area, arb. units	Peak area, %	Substance
1	1.26	7474388	2.24	Butane
2	1.376	32279339	9.68	Acetaldehyde
3	1.512	49558420	14.86	Acetaldehyde, dimethylacetal
4	1.557	44096080	13.22	Acetone
5	1.619	4877081	1.46	Acetaldehyde, ethylmethylacetal
6	1.71	31176492	9.35	Propionaldehyde, dimethylacetal
7	1.817	4605863	1.38	2-Butanone
8	1.85	2030641	0.61	<i>tert</i> -Butyl alcohol
9	1.924	25480558	7.64	Isopropyl alcohol
10	1.961	6490246	1.95	Ethanol
11	2.056	1868478	0.56	Methylvinylketone
12	2.13	3015494	0.9	Isobutylaldehydedimethylacetal
13	2.167	1960131	0.59	—
14	2.188	1431138	0.43	2-Pentanol, 2,3-dimethyl-
15	2.241	2649206	0.79	2-Pentanone
16	2.365	1221583	0.37	—
17	2.443	3201569	0.96	<i>tert</i> -Amyl alcohol
18	2.46	1247459	0.37	Acetonitrile
19	2.583	36373198	10.91	2-Butanol
20	2.732	5448223	1.63	1-Propanol
21	2.827	540174	0.16	1,3-Butadien-1-ol
22	2.872	5653988	1.7	2-Butanol, 3-methoxy-
23	3.235	4428273	1.33	3-Buten-2-ol
24	3.395	2839110	0.85	2-Butanol, 3-methoxy-
25	3.42	1947805	0.58	Isobutanol
26	3.507	1337671	0.4	2-Pentanol, 2-methyl-
27	3.618	2197485	0.66	Neoamyl alcohol
28	3.742	779003	0.23	Allyl alcohol
29	3.787	677954	0.2	2-Butanol, 3-methyl-
30	3.907	674332	0.2	1-Propanol, 2-ethoxy-
31	4.179	3988175	1.2	1-Butanol
32	4.414	1873813	0.56	1-Nitro-2-propanol
33	4.974	988046	0.3	3-Hexanol, 3-methyl-
34	5.201	2311254	0.69	2-Buten-1-ol
35	5.267	2344686	0.7	2-Methyl-2-pentanol
36	5.399	821819	0.25	<i>trans</i> -Crotonyl alcohol
37	6.59	7554713	2.27	Acetoin
38	6.87	4966675	1.49	<i>N,N</i> -Dimethylformamide
39	7.089	3670317	1.1	<i>tert</i> -Butyl hydroperoxide
40	8.02	764183	0.23	1-Hydroxy-2-butanone
41	8.498	1004345	0.3	—
42	9.261	11863305	3.56	Acetic acid
43	10.403	1704348	0.51	1,2-Butanediol
44	10.526	976075	0.29	Propanoic acid
45	10.942	752234	0.23	Propanoic acid, 2-methyl-
46	11.738	316571	0.09	Butanoic acid

REFERENCES

1. V. S. Arutyunov, V. I. Savchenko, and M. Yu. Sinev, *Gaz. Biznes*, No. 3, 24 (2011).
2. V. D. Rusanov and A. A. Fridman, *Physics of Chemically Active Plasma* (Nauka, Moscow, 1981) [in Russian].
3. A. I. Pushkarev and G. E. Remnev, *Applied Plasma Chemistry* (TPI, Tomsk, 2011) [in Russian].
4. E. Tana, S. Unala, A. Doganb, et al., *Radiat. Phys. Chem.* **119**, 109 (2016).
5. A. Basfar, I. Fageeha, N. Kunnummal, et al., *Fuel* **87**, 1446 (2008).
6. J. Kim, Y. Kim, B. Han, et al., *J. Korean Phys. Soc.* **59**, 3494 (2011).
7. A. I. Pushkarev, A. M. Zhu, X.-S. Li, and R. V. Sazonov, *High Energy Chem.* **43**, 156 (2009).
8. E. Tatarova, N. Bundaleska, J. Ph. Sarrette, and C. M. Ferreira, *Plasma Sources Sci. Technol.* **23**, 063002 (2014).
9. Ph. G. Rutberg, A. N. Bratsev, V. A. Kuznetsov, et al., *Tech. Phys. Lett.* **40**, 725 (2014).
10. X. Tao, M. Bai, H. Long, et al., *Prog. Energy Combust. Sci.* **37**, 113 (2011).
11. R. G. Sharafutdinov, E. E. Son, S. V. Alekseenko, et al., in *Proceedings of XXXII International Conference on Phenomena in Ionized Gases* (Iasi, Romania, 2015).
12. R. G. Sharafutdinov, P. A. Skovorodko, S. A. Gorodetskii, et al., RU Patent No. 2612267 (2015).
13. A. N. Zvilopulo, M. I. Mykyta, A. N. Mylymko, and O. B. Shpenik, *Tech. Phys.* **83**, 1251 (2013).

Translated by S. Zatonsky